Fused Donor–Acceptor Ligands in RuII Chemistry: Synthesis, Electrochemistry and Spectroscopy of [Ru(bpy)3–n(TTF-dppz)n](PF6)2

ARTICLE *in* CHEMPHYSCHEM · JULY 2007

Impact Factor: 3.42 · DOI: 10.1002/cphc.200700066 · Source: PubMed

7 AUTHORS, INCLUDING:

Christine Goze
University of Burgundy
49 PUBLICATIONS **1,148** CITATIONS
SEE PROFILE

Shi-Xia Liu
Universität Bern
127 PUBLICATIONS **1,925** CITATIONS
SEE PROFILE

Lionel Sanguinet
University of Angers
48 PUBLICATIONS **849** CITATIONS
SEE PROFILE

Silvio Decurtins
Universität Bern
273 PUBLICATIONS **6,350** CITATIONS
SEE PROFILE

CHEMPHYSCHEM

DOI: 10.1002/cphc.200700066

Fused Donor–Acceptor Ligands in Ru^{II} Chemistry: Synthesis, Electrochemistry and Spectroscopy of $[Ru(bpy)_{3-n}(TTF\text{-}dppz)_n](PF_6)_2$**

Christine Goze,[a] Claudia Leiggener,[b] Shi-Xia Liu,*[a] Lionel Sanguinet,[c] Eric Levillain,[c] Andreas Hauser,*[b] and Silvio Decurtins[a]

Three ruthenium(II) polypyridine complexes of general formula $[Ru(bpy)_{3-n}(TTF\text{-}dppz)_n](PF_6)_2$ (n = 1-3, bpy = 2,2′-bipyridine), with one, two or three redox-active TTF-dppz (4′,5′-bis(propylthio)tetrathiafulvenyl[i]dipyrido[3,2-a:2′,3′-c]phenazine) ligands, were synthesised and fully characterised. Their electrochemical and photophysical properties are reported together with those of the reference compounds $[Ru(bpy)_3](PF_6)_2$, $[Ru(dppz)_3](PF_6)_2$ and $[Ru(bpy)_2(dppz)](PF_6)_2$ and the free TTF-dppz ligand. All three complexes show intraligand charge-transfer (ILCT) fluorescence of the TTF-dppz ligand. Remarkably, the complex with n = 1 exhibits luminescence from the $Ru^{2+}\rightarrow$dppz metal-to-ligand charge-transfer (^{3}MLCT) state, whereas for the other two complexes, a radiationless pathway via electron transfer from a second TTF-dppz ligand quenches the ^{3}MLCT luminescence. The TTF fragments as electron donors thus induce a ligand-to-ligand charge-separated (LLCS) state of the form $TTF\text{-}dppz^{-}\text{-}Ru^{2+}\text{-}dppz\text{-}TTF^{+}$. The lifetime of this LLCS state is approximately 2.3 μs, which is four orders of magnitude longer than that of 0.4 ns for the ILCT state, because recombination of charges on two different ligands is substantially slower.

Introduction

Materials science has made rapid progress, stimulated by interest in elucidating structure–function relationships at the molecular level. In the more specific context of molecular conductors, a distinct class of compounds, namely, functionalised tetrathiafulvalenes (TTFs), plays a unique role.[1] Because of their specific π-donor properties, TTFs have been incorporated into a number of macrocyclic, molecular and supramolecular systems to create multifunctional materials with desired structures, stability and physical properties.[2–4] Considerable efforts are currently devoted to modification of the TTF core with substituents such as pyridine-type heterocycles,[5] dithiolates,[6] acetylacetonates[7] and phosphines,[8] all of which are well-tailored for chelation of various transition metal ions. Recently, it was demonstrated that such electroactive ligands allow access to dual-property molecular materials in which close vicinity of a metal centre to a $TTF^{\bullet+}$ radical leads to enhanced d–π interactions.[9] Subsequently, we reported an efficient synthetic route to an annulated donor–acceptor (D–A) ensemble, namely, 4′,5′-bis(propylthio)tetrathiafulvenyl[*i*]dipyrido-[3,2-*a*:2′,3′-*c*]phenazine (TTF-dppz, Figure 1).[10] This new chelating ligand has two redox centres and shows fascinating photophysical properties in its own right. For instance, the first electronically excited state corresponds to a TTF→dppz intraligand charge-transfer (ILCT) state, from which corresponding CT fluorescence is observed. But of course, it also invites investigation of its coordination behaviour toward redox-active metal ion centres, such as ruthenium(II).

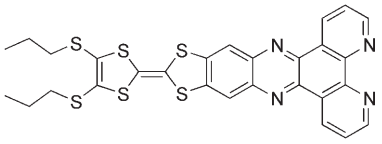

Figure 1. Structure of the TTF-dppz ligand.

Ruthenium(II) polypyridine complexes have been intensively investigated owing to their interesting photophysical properties and their chemical stability. Notably, they offer a predictable design strategy for building up rigid chiral structures spanning all three spatial dimensions.[11] An intriguing part of their chemistry lies in a variety of fields related to solar-energy con-

[a] *Dr. C. Goze, Dr. S.-X. Liu, Prof. S. Decurtins*
Departement für Chemie und Biochemie
Universität Bern
Freiestrasse 3, 3012 Bern (Switzerland)
Fax: (+41) 31-6313995
E-mail: liu@iac.unibe.ch

[b] *Dr. C. Leiggener, Prof. A. Hauser*
Département de chimie physique
Université de Genève, 30 quai Ernest-Ansermet
1211 Genève 4 (Switzerland)
Fax: (+41) 22-37-96103
E-mail: Andreas.Hauser@chiphy.unige.ch

[c] *Dr. L. Sanguinet, Dr. E. Levillain*
Chimie, Ingénierie Moléculaire et Matériaux d'Angers
UMR 6200 du CNRS - 2 bd Lavoisier, 49045 Angers Cedex (France)

[**] n = 1–3, TTF-dppz = 4′,5′-bis(propylthio)tetrathiafulvenyl[*i*]dipyrido[3,2-*a*:2′,3′-*c*]phenazine.

Supporting information for this article is available on the WWW under http://www.chemphyschem.org or from the author.

version and photochemistry.[12] In particular, they act as photosensitisers in the conversion of solar energy to chemical or electrical energy, whereby a major achievement has been the development of a dye-sensitised solar cell by Grätzel and coworkers.[13] Furthermore, ruthenium(II) complexes containing the dipyrido[3,2-*a*:2′,3′-*c*]phenazine (dppz) ligand have emerged as one of the most promising metal-ion-based molecular probes of DNA because of their unique emission properties arising from extended aromatic structures incorporating a phenazine moiety.[14–16]

Incorporation of the TTF unit into ruthenium(II) complexes is stimulated by the development of new antenna and charge-separation systems[17] and photoredox switches.[18,19] Among the reported examples, the TTF moiety is linked to the ruthenium(II) chromophore via diimine coordination or through an N,S chelating ligand. In the former cases, luminescence from metal-to-ligand charge-transfer (MLCT) states is strongly quenched by intramolecular electron transfer from the pendant TTF unit, which makes them promising candidates for incorporation into optical sensors and devices.

Thus, the TTF-dppz ligand, when coordinated in metal complexes, generates unique supramolecular assemblies with multielectron redox and photophysical properties. The hybrid complexes with a polypyridylruthenium(II) centre could be particularly interesting, because they have two types of emissive chromophores directly connected to each other. Therefore, we prepared $[Ru(bpy)_{3-n}(TTF\text{-}dppz)_n](PF_6)_2$ complexes (**1** $n=1$; **2** $n=2$; **3** $n=3$) containing one, two or three TTF-dppz ligands and investigated their electrochemical and photophysical properties with the purpose of studying how the TTF-fused dppz ligand affects the redox and photophysical properties of ruthenium(II) polypyridyl moieties.

Results and Discussion

Synthesis

Complex **1** can be synthesised in two different ways (Scheme 1). Coordination of the TTF-dppz ligand to $[Ru(bpy)_2Cl_2]$ forms the target compound in fair yield. This method is convenient for introducing diimine ligands with good solubility in common organic solvents into Ru^{II} polypyridyl complexes. The alternative approach involving condensation of a diaminofunctionalised TTF ligand with $[Ru(bpy)_2(phendione)]^{2+}$ also affords **1** in good yield. In this case, the solubility problems that are often encountered when incorporating rigid and planar diimine ligands into extended mononuclear and polynuclear systems can be avoided. By following the second strategy, complexes **2** and **3** (Scheme 2) were obtained in reasonable yields.

All compounds were unambiguously characterised by elemental analysis and standard spectroscopic techniques. The ^1H NMR spectra display characteristic peaks for protons of the aromatic rings and also two triplets at 2.76 and 0.95 ppm and one multiplet for the propyl groups of the TTF-dppz unit(s). The ESI-MS spectra reveal a major peak corresponding to $[M-PF_6]^+$ for **1** and $[M-2PF_6]^{2+}$ for **2** and **3**.

Electrochemistry

The electrochemical properties of **1**–**3** were investigated by cyclic voltammetry. Their electrochemical data are collected in Table 1 together with those of $[Ru(bpy)_3]^{2+}$, $[Ru(bpy)_2(dppz)]^{2+}$ and $[Ru(dppz)_3]^{2+}$ for comparison.

As shown in Figures 2 and 3, in CH_2Cl_2/CH_3CN (5:1) **1** and **2** undergo three reversible oxidation processes. In pure CH_2Cl_2, only the first two are reversible, and the last one shows evidence of an adsorption phenomenon, which can be avoided by the addition of a small amount of CH_3CN (Figure 2). In **1** all

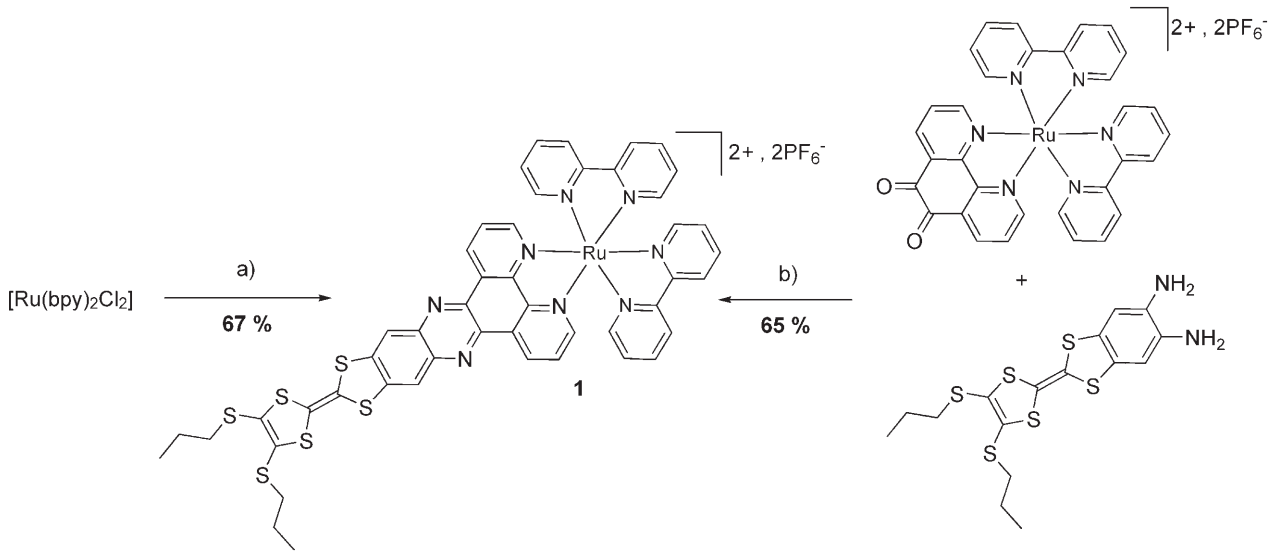

Scheme 1. Synthesis of **1**. a) TTF-dppz, $EtOH/H_2O$, heating at reflux, 16 h. b) EtOH, heating at reflux, 16 h.

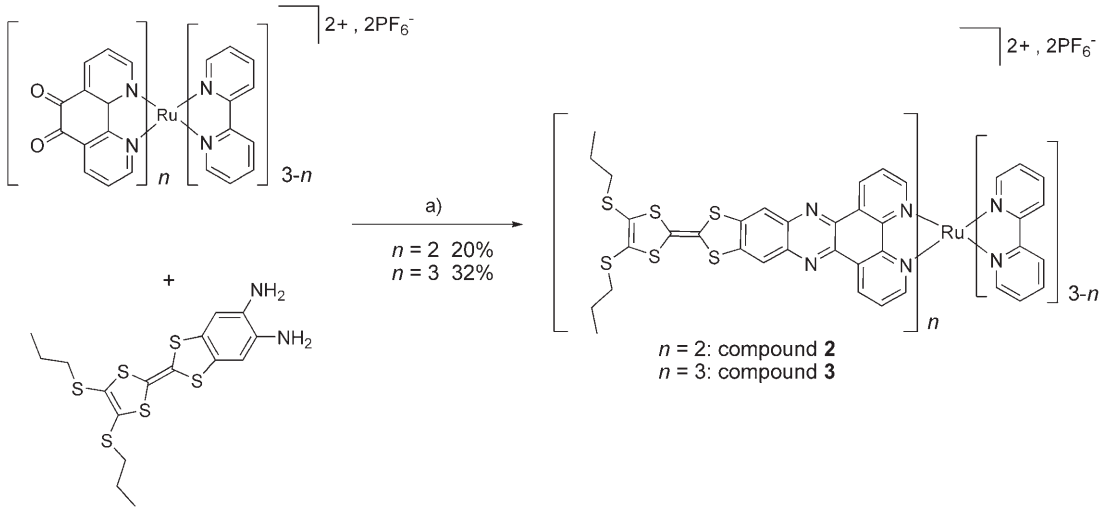

Scheme 2. Synthesis of **2** and **3**. a) EtOH, heating at reflux, 16 h.

Table 1. Redox potentials (V vs. Fc/Fc^+) of **1**–**3** in CH_2Cl_2/CH_3CN (5:1) and of the reference compounds $[Ru(bpy)_3]^{2+}$, $[Ru(dppz)_3]^{2+}$ and TTF-dppz in CH_2Cl_2, $[Ru(bpy)_2(dppz)]^{2+}$ in CH_3CN.[20]

Compound	$E_{1/2}^{ox1}$	$E_{1/2}^{ox2}$	$E_{1/2}^{ox3}$	$E_{1/2}^{red1}$	$E_{1/2}^{red2}$
$[Ru(bpy)_3]^{2+}$			0.93	−1.72	−1.99
$[Ru(bpy)_2(dppz)]^{2+}$			0.91	−1.36	−1.79
$[Ru(dppz)_3]^{2+}$			1.11	−1.43	
TTF-dppz	0.29	0.64		−1.61	
1	0.29	0.61	0.99	−1.35[a]	−1.79[a]
2	0.30	0.65	1.07	−1.37[a]	−1.94[a]
3	0.31	0.66	1.17	−1.30[b]	

[a] In CH_2Cl_2. [b] Irreversible in CH_2Cl_2.

three oxidations correspond to one-electron processes, while in **2** the first two are two-electron processes and only the third is a one-electron process (Figure 3). The first two oxidation processes for both complexes can be assigned to the TTF subunits, while the third corresponds to the $Ru^{II/III}$ redox couple. No splitting was observed in the first oxidation wave of **2**. Compared to **1**, the oxidation waves of **2** are positively shifted by 10, 40 and 80 mV, respectively, owing to the electron-withdrawing effect of the dppz moieties. The positive shift in the metal-centred oxidation process on going from **1** to **3** is not unexpected on the basis of simple electrostatic arguments; the TTF units are oxidised first.

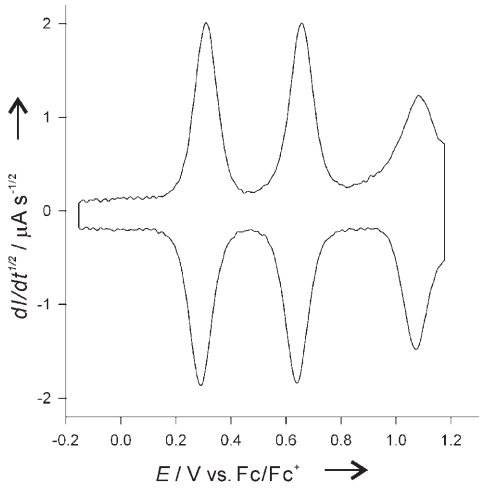

Figure 3. Deconvoluted cyclic voltammogram of **2** in CH_2Cl_2/CH_3CN (5:1).

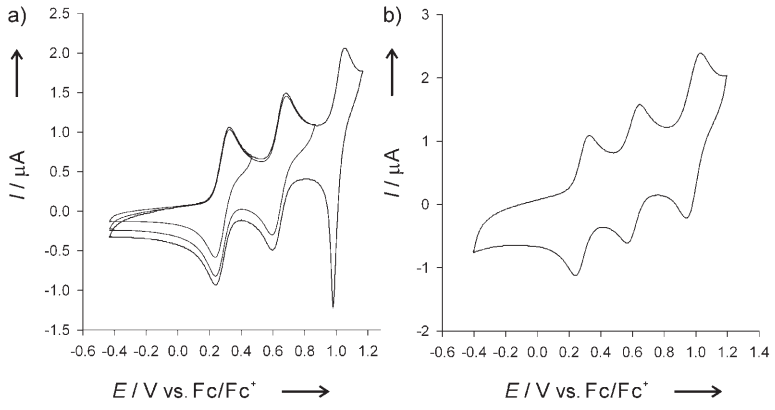

Figure 2. Cyclic voltammograms of **1** in a) CH_2Cl_2 and b) CH_2Cl_2/CH_3CN (5:1).

Complex **3** shows a significantly different electrochemical behaviour than **1** and **2**. Two reversible multi-electron oxidation waves for the oxidation of the three TTF fragments were observed (Figure 4a). The first oxidation wave is broad and shows some splitting, which suggests that the three TTF units in **3** can be oxidised successively to the cation-radical states. This splitting also indicates possible intramolecular electronic interactions among TTF moieties, as previ-

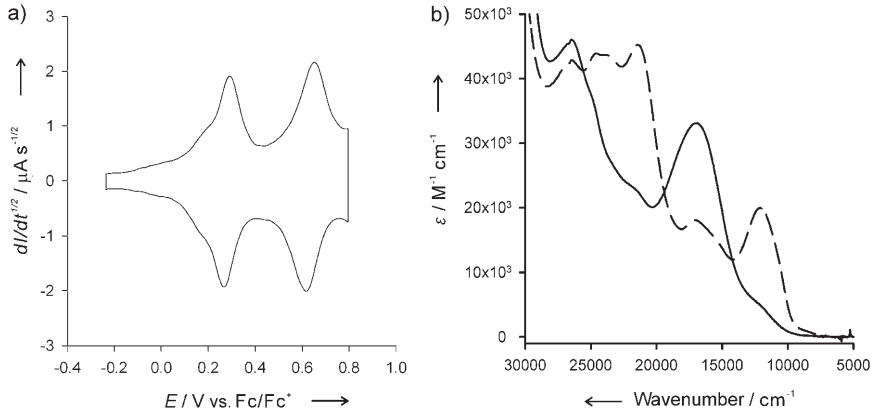

Figure 4. a) Deconvoluted cyclic voltammogram of **3** in CH_2Cl_2/CH_3CN (5:1). b) Evolution of the absorption spectrum of **3** in CH_2Cl_2/CH_3CN (5:1) without (solid) and with addition of aliquots of $NOSbF_6$ (dashed, 3 oxidation equivalents).

ously observed in the related TTF-HAT (HAT = hexaazatriphenylene) molecule, for which intramolecular through-bond interactions among the three TTF units were electrochemically detected.[21] A corresponding UV/Vis/NIR spectroelectrochemical investigation of **3** was performed (NIR = near infrared). However, no intervalence absorption bands due to possible formation of mixed-valent species could be observed in the NIR region. The chemical oxidation of **3** only gives rise to new absorption bands at 466 and 845 nm (11 830 and 21 460 cm^{-1}), which are characteristic of the cation-radical species (Figure 4b). In addition, the Ru$^{II/III}$ redox couple is shifted to even more positive potential compared to **2**, which is in agreement with a further decrease in electron density around Ru^{II} caused by the π-acceptor properties of the dppz subunits.

At negative potentials, two reversible reduction waves were observed for **1** and **2** (Table 1 and Figure 5), which represent reduction of the dppz and bpy moieties. In **2**, the first reduction process corresponds to reduction of two dppz units with one electron each. The negative shift of the second reduction potential of **2** is attributable to the presence of two reduced dppz units in the molecule. In the case of **3**, the reduction process is irreversible. Since the first reduction processes in complexes **1**–**3** take place at potentials that are less negative than those of bpy, the lowest unoccupied molecular orbital (LUMO) in each case must reside on the dppz unit(s).

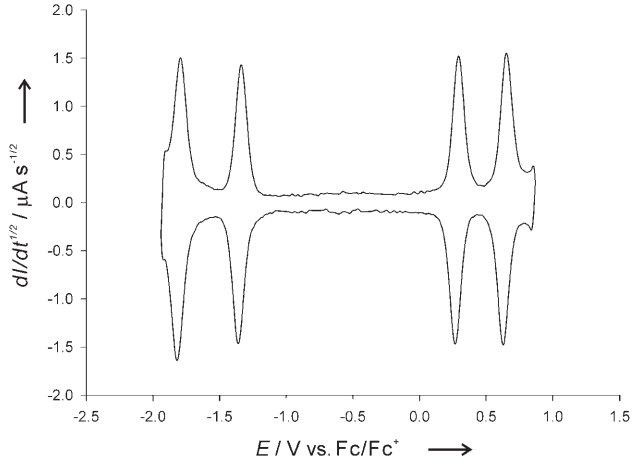

Figure 5. Deconvoluted cyclic voltammogram of **1** in CH_2Cl_2.

Optical Properties

The absorption spectra of the three complexes **1**–**3** in dichloromethane, together with that of $[Ru(bpy)_3](PF_6)_2$, are presented in Figure 6. By comparison with the absorption spectra of the reference compounds

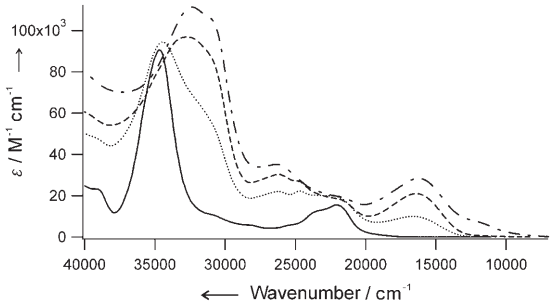

Figure 6. Absorption spectra of **1** (dots), **2** (dash), **3** (dash-dots) and $[Ru(bpy)_3](PF_6)_2$ (solid line) in CH_2Cl_2.

$[Ru(bpy)_2(dppz)](PF_6)_2$ and $[Ru(dppz)_3](PF_6)_2$ as well as of the free TTF-dppz ligand[10] in dichloromethane (see the Supporting Information), the absorption bands can be readily attributed to specific transitions.

The broad band at 16 180 cm^{-1} corresponds to an ILCT transition on TTF-dppz, with the TTF subunit acting as an electron donor and the dppz subunit as an acceptor. With respect to the free ligand, this ILCT absorption band is red-shifted by 2320 cm^{-1}, because the energy of the LUMO localised on the dppz unit is lowered upon coordination to ruthenium(II). This shift is in good agreement with that observed in the corresponding zinc(II)- and iron(II)-coordinated systems.[10] The extinction coefficient of the ILCT band increases from 1×10^4 to 3×10^4 M^{-1}cm^{-1} on going from one to three TTF-dppz ligands per complex. As expected, electric-dipole-allowed MLCT transitions around 21 900 cm^{-1} are also observed, that is, both $Ru^{2+}\rightarrow$bpy and $Ru^{2+}\rightarrow$dppz transitions. In particular, the peak positions, the broadness and the intensities of the ^{1}MLCT absorption bands of **1**–**3** and the reference complexes (see the Supporting Information) do not change markedly with increasing number of dppz moieties, that is, the $Ru^{2+}\rightarrow$bpy and $Ru^{2+}\rightarrow$dppz transitions are close to each other in energy.

The absorption band centred at 26200 cm^{-1} can be assigned to π–π* transitions located on the dppz subunit. It is slightly red-shifted compared to the free TTF-dppz ligand. Again the extinction coefficient increases with increasing number of TTF-dppz ligands per complex. In the UV region, a broad band is attributed to several overlapping π–π* transitions located on the TTF and dppz subunits as well as on the bpy ligand.

All three complexes **1**–**3** show rather weak photoluminescence around 10800 cm^{-1} (920 nm) in dichloromethane, which is depicted in Figure 7 for complex **1**, and which can be assigned to the ILCT fluorescence of the TTF-dppz ligand.[10] The emission intensity does not vary much among the different complexes but drops to around 20% of the intensity of non-coordinated TTF-dppz, which shows fluorescence at 12198 cm^{-1} (820 nm) with a lifetime of 450 ps and a quantum efficiency of about 1% in dichloromethane at room temperature. The decrease in luminescence intensity which occurs upon complexation can be explained by the smaller energy gap and faster nonradiative decay according to the energy-gap law in the Marcus inverted region. By using the semiclassical theory[22] with an average accepting mode corresponding to the skeletal vibrational modes of the TTF and phenazine units between 1000 and 1500 cm^{-1},[23] a decrease in the driving force from 15350 cm^{-1} for the free ligand to 13100 cm^{-1} for the coordinated system (estimated from the crossing point of the respective absorption and emission spectra[10] in Figure 7), and a total reorganisation energy of approximately 3200 cm^{-1} (half of which is attributed to the local modes), the increase in the nonradiative rate constant is estimated to be on the order of a factor of ten. Additional quenching mechanisms can thus be excluded. Therefore, the lifetime of the ILCT state in the complexes **1**–**3** can be estimated as $\tau_{ILCT} \approx 100$ ps.

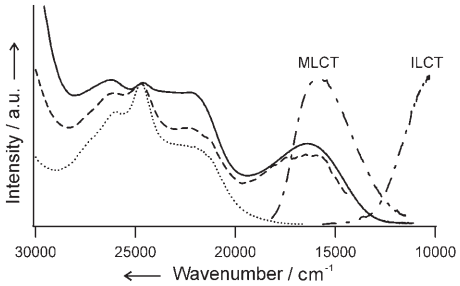

Figure 7. Absorption (solid line), emission (dash-dots) and excitation (dots and dashed line) spectra of **1** in CH_2Cl_2. For the luminescence spectra, the sample was excited at 21739 cm^{-1} (460 nm) and at 16666 cm^{-1} (600 nm). The excitation spectrum of the MLCT luminescence (dots) was detected at 15873 cm^{-1} (630 nm), and the excitation spectrum of the ILCT fluorescence (dashed) at 10638 cm^{-1} (950 nm).

In addition, complex **1** shows a quite intense ^{3}MLCT luminescence band centred at 16181 cm^{-1} (618 nm), as depicted in Figure 7. Its lifetime and quantum efficiency are 1040(1) ns and 0.014(2), respectively. This ^{3}MLCT luminescence is strongly quenched in **2** and **3**. The relevant spectroscopic results, including those for the reference complexes, are summarised in Table 2. Compared to $[Ru(bpy)_2(dppz)]^{2+}$ (the reference complex without TTF), the luminescence lifetime of complex **1** is longer, whereas the quantum yield is lower; this situation results in somewhat different radiative and nonradiative rate constants. The enhanced rigidity of the dppz acceptor arising from the annulation of TTF appears to play a role in the electronic nature of the emitting ^{3}MLCT state, as demonstrated by other reported examples.[24] Interestingly, the TTF fragment does not act as an efficient electron-transfer quencher of the MLCT luminescence in **1**, in contrast to **2, 3** and a number of related ruthenium(II) complexes.[17] The question that now arises concerns the nature of the emitting ^{3}MLCT state in **1** and why only this complex shows ^{3}MLCT luminescence.

Table 2. Photophysical data[a] for the ^{3}MLCT luminescence of **1**–**3** and the reference complexes in CH_2Cl_2 at room temperature.

Complex	λ_{max} [nm]	I_{em} [%]	Φ_{em}	τ [ns]	k_r [s^{-1}]	k_{nr} [s^{-1}]
$[Ru(bpy)_3]^{2+}$	604	100	0.029	486(2)	6×10^4	2×10^6
$[Ru(bpy)_2(dppz)]^{2+}$	606	153	0.044(6)	606(1)	7.4×10^4	1.6×10^6
$[Ru(dppz)_3]^{2+}$	596	71	0.021(3)	250(1)	8.2×10^4	3.9×10^6
1	618	47	0.014(2)	1040(1)	1.3×10^4	9.6×10^5
2	608	2	–	–		
3	604	<1	–	–		

[a] λ_{max}: luminescence maximum, I_{em}: luminescence intensity relative to $[Ru(bpy)_3]^{2+}$, Φ_{em}: luminescence quantum yield (λ_{ex} = 460 nm). τ: measured luminescence lifetime, k_r: radiative rate constant, k_{nr}: nonradiative rate constant.

A helpful indication is provided by the excitation spectra. In contrast to those of reference complex $[Ru(bpy)_2(dppz)]^{2+}$ and free TTF-dppz, which are identical to their absorption spectra (see the Supporting Information), the excitation spectra of **1** shown in Figure 7 depend on the detection wavelength and differ from the absorption spectrum. In particular, the absence of some allowed MLCT bands from the excitation spectra suggests that there are allowed transitions to ^{1}MLCT states which relax neither to the emitting ^{3}MLCT state nor to the ILCT state. Instead, they relax nonradiatively to a lower excited dark state or to the ground state. As mentioned above, the $Ru^{2+}\rightarrow$bpy and $Ru^{2+}\rightarrow$dppz ^{1}MLCT states are close to each other in energy, but it is generally acknowledged that the lowest emissive ^{3}MLCT state in solution is the $Ru^{2+}\rightarrow$dppz state.[25] Excitation to specific π–π* transitions of dppz, represented by the sharp band at 24700 cm^{-1}, however, results in efficient relaxation to the luminescent ^{3}MLCT state as well as to the fluorescent ILCT state. In addition to the MLCT and ILCT states and according to the electrochemical data (Table 1), ligand-to-ligand charge-separated (LLCS) states at comparatively low energies must be considered for a complete energy-level diagram. With regard to electron-transfer quenching, both TTF$\rightarrow Ru^{3+}$ and TTF$\rightarrow$L (L = bpy.dppz) processes may be operative.

Accordingly, the energy-level diagrams for **1** and **3** are depicted in Scheme 3. An analogous diagram for **2** is obtained by combining those of **1** and **3**; that is, **2** has two different ^{1}MLCT states like **1**, two different LLCS states corresponding to the LLCS states of **1** and **3**, respectively, and one ILCT state. Generally, the first electronic excited states in all complexes are the ILCT and LLCS states, while the MLCT states lie higher in

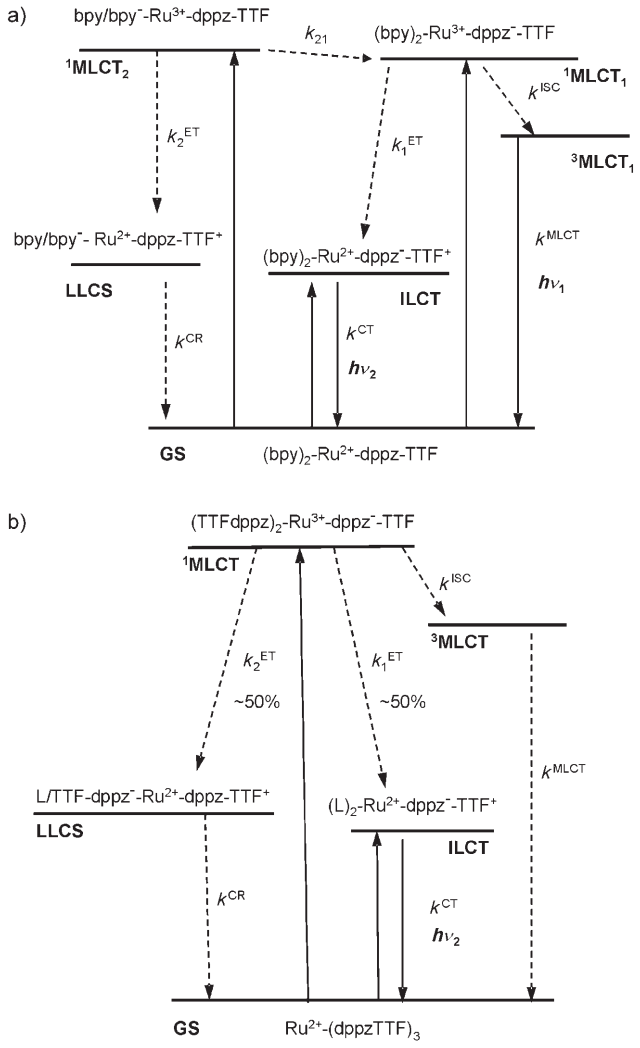

Scheme 3. Energy-level schemes for the CT states of **1** (a) and **3** (b). L stands for the neutral TTF-dppz ligand. The different rate constants are explained in the text.

energy. Complexes **1** and **2** both have two almost isoenergetic ^{1}MLCT states, namely, Ru^{2+}→dppz (^{1}MLCT$_1$) and Ru^{2+}→bpy (^{1}MLCT$_2$), which interact only weakly with each other but can transform into each other by interligand electron hopping (k_{21}). Complex **1** shows luminescence from the ^{3}MLCT$_1$ state with a decay rate k^{MLCT} of 9.6×10^5 s^{-1}, as well as ILCT fluorescence. The excitation spectra in Figure 7 indicate that the ILCT state can be excited either directly or via the ^{1}MLCT$_1$ state. In the latter case, electron transfer from TTF to ruthenium(III) to form the ILCT state (bpy)$_2$-Ru^{2+}-dppz$^-$-TTF$^+$ must be comparatively slow, since it does not quench the ^{3}MLCT$_1$ luminescence substantially. In other words, the rate constant k_1^{ET} is on the order of the rate constant for intersystem crossing k^{ISC}, that is, around 10^{11} s^{-1}.[26] The analogous ^{1}MLCT$_2$ state, however, relaxes rapidly to the charge-separated LLCS state bpy/bpy$^-$-Ru^{2+}-dppz-TTF$^+$ by electron transfer. This is concluded from the missing part of the excitation spectrum in Figure 7. Rate constant k_2^{ET} is expected to be on the order of 10^{12} s^{-1}, because it must compete with fast interligand randomisation of the ^{1}MLCT states, which is known to occur in a few picoseconds.[27]

For **2** and **3**, ILCT fluorescence similar to that of **1** is observed, but there is no ^{3}MLCT luminescence. The energy-level diagrams of these complexes have almost isoenergetic LLCS states, namely, L/TTF-dppz$^-$-Ru^{2+}-dppz-TTF$^+$ (L = bpy for **2** and TTF-dppz for **3**), in which the charges are located on two different TTF-dppz ligands. This LLCS state cannot be populated by direct excitation from the ground state, but it can be formed by electron transfer in the excited state, that is, an electron from another TTF-dppz ligand is transferred to the formally Ru^{3+} ion, and a TTF$^+$ radical is formed on this ligand. The fact that the ^{3}MLCT luminescence is strongly quenched in **2** and **3** but not in **1** indicates that this kind of electron transfer can occur as soon as a second TTF-dppz ligand is available. The rate constant of this process k_3^{ET} is expected to be a bit larger than k^{ISC}. For **3**, the quantum efficiency for population of the ILCT state after excitation to the ^{1}MLCT state was determined to be around 50%. Owing to the lack of ^{3}MLCT luminescence in **3**, it is suggested that the other 50% relaxes to the LLCS state. In principle, the driving force for both electron-transfer processes ET$_1$ (k_1^{ET}) and ET$_3$ (k_3^{ET}) is given by the difference between the reduction potentials of Ru^{3+} and TTF$^+$, that is, around 0.7 eV (Table 1). Mechanistically, one can assume that $k_3^{ET} > k_1^{ET}$ because of the Coulomb barrier provided by the negative charge located on dppz$^-$ between the formally Ru^{3+} ion and the TTF unit for the ET$_1$ process.

Population of the LLCS states after excitation to the ^{1}MLCT states was demonstrated by means of transient absorption spectroscopy on all three complexes. As an example, the transient absorption spectrum of **2** is shown in Figure 8 together with the ground-state absorption spectrum of the oxidised complex. Besides the bleaching of the ILCT ground-state absorption, there are two transient absorption bands around 20000 and 12000 cm^{-1}, which are in good agreement with the absorption bands of TTF$^+$. In particular, the band at 12000 cm^{-1} can be assigned to the reversed ILCT transition of the oxidised form of the ligand (dppz→TTF$^+$).[10] This result means that the excited electron must be located on another TTF-dppz or bpy ligand. In fact, the low-energy part of the

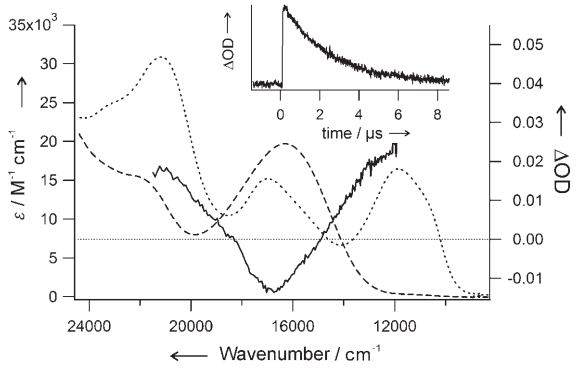

Figure 8. Transient absorption spectrum (solid line, ΔOD = change in optical density) and ground-state absorption spectra before (dash) and after (dots) chemical oxidation of complex **2** in CH_2Cl_2. The inset shows the decay of the transient signal detected at 800 nm (12000 cm^{-1}).

transient absorption band at 20000 cm^{-1} could be assigned to the absorption of bpy^- and $dppz^-$ radicals.[28]

The same transient absorption bands were also observed for **1** and **3**. This shows that the LLCS state bpy^--Ru^{2+}-dppz-TTF^+ and the LLCS state TTF-$dppz^-$-Ru^{2+}-dppz-TTF^+ are populated after excitation to the corresponding ^{1}MLCT state. The lifetimes of the LLCS states are 2.45 and 2.26 μs, respectively (see Table 3). In **2**, both states may be populated, but they cannot be distinguished due to the very similar lifetimes. The charge-recombination process was found to follow first-order kinetics in all three complexes. Within the detection timescale of the system used for the measurements (5-ns laser pulse), no rise of the signal after excitation was observed, which is in agreement with the abovementioned fast electron-transfer process from TTF to ruthenium(III).

Table 3. Lifetimes of the LLCS states of **1**–**3** in CH_2Cl_2 at room temperature. The signals were detected at 800 nm.

Complex	k^{CR}[a] [s^{-1}]	τ[b] [μs]
1	$4.08(8)\times10^5$	2.45(5)
2	$4.20(5)\times10^5$	2.38(3)
3	$4.42(8)\times10^5$	2.26(4)

[a] Rate constant for charge recombination. [b] Lifetime.

Conclusions

A new synthetic protocol for the preparation of Ru^{II} bipyridine complexes bearing multiple appended TTF fragments has been presented. On the basis of the photophysical results, all of the compounds display a characteristic ILCT excited state. Interestingly, the compound containing only one TTF-dppz ligand exhibits dual luminescence. However, in cases where two or three TTF-dppz ligands are present in the structures, the ^{3}MLCT luminescence is strongly quenched due to electron transfer from a second TTF-dppz ligand to Ru^{3+} to form a charge-separated state TTF-$dppz^-$-Ru^{2+}-dppz-TTF^+. The lifetime of this LLCS state is approximately 2.3 μs at room temperature in dichloromethane. An analogous LLCS state in which the negative charge is located on a bipyridine ligand, namely, bpy^--Ru^{2+}-dppz-TTF^+, was also detected for the complex with only one TTF-dppz ligand. Its lifetime is 2.5 μs in dichloromethane. For this complex there are, therefore, three different mechanisms for deactivation of the excited ^{1}MLCT states, which are observed simultaneously. Either intersystem crossing to the $Ru^{2+}\rightarrow$dppz ^{3}MLCT state and subsequent phosphorescence ($\tau = 1$ μs) occurs, or electron transfer out of the $Ru^{2+}\rightarrow$dppz ^{1}MLCT state to the ILCT state followed by fluorescence or electron transfer out of the $Ru^{2+}\rightarrow$bpy ^{1}MLCT state to populate the LLCS state takes place.

In essence, the electron-donating properties of the TTF component of the diimine ligand results in ILCT and LLCS states at low energies relative to the MLCT states. The current work illustrates that, with appropriately substituted ligands, ruthenium(II) complexes can generate a long-lived charge-separated state at room temperature, which is quite unique. Such molecules are of interest because of their potential applications in optoelectronics as well as in the development of molecular probes for DNA.

Experimental Section

General Methods and Materials: Air- and water-sensitive reactions were conducted under argon in dry, freshly distilled solvents. Unless otherwise stated, all reagents were purchased from commercial sources and used without additional purification. 4′,5′-Bis-(propylthio)tetrathiafulvenyl[*i*]dipyrido[3,2-*a*:2′,3′-*c*]phenazine (TTF-dppz),[10] $[Ru(bpy)_2Cl_2]$,[29] 5,6-diamino-2-[4,5-bis(propylthio)-1,3-dithio-2-ylidene]benzo[*d*]-1,3-dithiole,[10,21] $[Ru(bpy)_2(phendione)](PF_6)_2$,[25] $[Ru(bpy)(phendione)_2](PF_6)_2$[30] and $[Ru(phendione)_3](PF_6)_2$[31] were prepared according to literature procedures. Elemental analyses were performed on an EA 1110 Elemental Analyzer CHN Carlo Erba Instruments. FTIR spectra were recorded on a Perkin-Elmer One FTIR spectrometer.

Cyclic Voltammetry: Cyclic voltammetry (CV) was performed in a three-electrode cell equipped with a platinum millielectrode, a platinum wire counter electrode and a silver wire as quasi-reference electrode. The electrochemical experiments were carried out in a dry and oxygen-free atmosphere ($H_2O < 1$ ppm, $O_2 < 1$ ppm) in CH_2Cl_2 (0.8 mM) with 0.1 M Bu_4NPF_6 (TBAP) as supporting electrolyte at 200 $mV\,s^{-1}$. The voltammograms were recorded on an EGG PAR 273A potentiostat with positive feedback compensation. Based on repetitive measurements, absolute errors in potentials were estimated to be about ±5 mV. The experimental voltammograms were deconvoluted with the CondeconTM software.

Photophysical Measurements: Photophysical measurements were performed on solutions of the compounds in CH_2Cl_2 [$c = (1–5)\times10^{-5}$ M] at room temperature. For luminescence and transient absorption measurements the solutions were degassed by bubbling N_2(g) through them for 30 min. Absorption spectra were recorded on a Variant Cary 5000 UV/Vis/NIR spectrophotometer. Emission and excitation spectra were measured on a Horiba Fluorolog 3 instrument. Luminescence lifetimes were measured by exciting the samples with the second harmonic (532 nm) of a pulsed Quantel Brilliant Nd:YAG laser. The system used for detection consisted of a Spex 270M monochromator, a Hamamatsu photomultiplier and a Tektronix TDS 540B oscilloscope. The signals were detected at 620 nm. For the transient absorption measurements, the samples were excited to the ^{1}MLCT state at 458 nm using a pulsed Nd:YAG laser system (Quantel Brilliant) with an integrated Magic Prism OPO and probed by a xenon lamp. The same system for detection was used as for the luminescence lifetime measurements.

Synthesis of $[Ru(bpy)_2(TTF\text{-}dppz)](PF_6)_2$ (**1**): TTF-dppz (80 mg, 0.16 mmol) was added to a stirred solution of $[Ru(bpy)_2]Cl_2$ (100 mg, 0.16 mmol) in ethanol/water (2:3, 50 mL). The mixture was heated for 16 h at 80 °C until complete consumption of the starting material was observed. After cooling to room temperature, the precipitate was filtered off. Aqueous potassium hexafluorophosphate was added to the filtrate. The crude precipitate was washed twice with water and once with diethyl ether and then purified by chromatography on a column packed with basic alumina ($MeOH/CH_2Cl_2$, gradient from 0:100 to 5:95). The fractions containing the pure complex were evaporated to dryness and recrystallised by slow evaporation of a solution in CH_2Cl_2/hexane (ca. 80:20) to give 140 mg (67%) of analytically pure product. ^{1}H NMR (CD_2Cl_2, 300 MHz): $\delta = 9.57$ [dd, $^3J(H,H) = 8.3$, $^4J(H,H) = 1.3$ Hz, 2H], 8.38 [t, ^3J-

(H,H) = 8.7 Hz, 4H], 8.12 (s, 2H), 8.08–8.02 (m, 4H), 7.95 [dt, ^3J(H,H) = 8.1, ^4J(H,H) = 1.5 Hz, 2H], 7.85 [dd, ^3J(H,H) = 8.3, ^3J(H,H) = 5.2 Hz, 2H], 7.77 [d, ^3J(H,H) = 5.6 Hz, 2H], 7.64 [d, ^3J(H,H) = 5.6 Hz, 2H], 7.49–7.44 (m, 2H), 7.29–7.25 (m, 2H), 2.76 [t, ^3J(H,H) = 7.2 Hz, 4H], 1.67–1.54 (m, 4H), 0.95 ppm [t, ^3J(H,H) = 7.3 Hz, 6H]; ^{13}C NMR (CD_2Cl_2, 75 MHz): δ = 157.6, 157.5, 153.8, 152.6, 152.54, 152.50, 152.4, 146.7, 139.8, 139.2, 139.0, 138.9, 134.8, 129.1, 129.0, 128.9, 128.5, 125.0, 124.9, 120.3 ppm; IR (KBr): $\tilde{\nu}$ = 2959, 1603, 1446, 1426, 1351, 1089, 838, 761, 557 cm^{-1}; UV/Vis (CH_2Cl_2): λ_{max} (ε) = 620 (9000), 453 (18000), 411 (21200), 385 nm (20000 $M^{-1}cm^{-1}$); ESI-MS: *m/z*: 1165.03, calcd for $[M-PF_6]^+$: 1165.02; 510.03, calcd for $[M-2PF_6]^{2+}$: 510.03; elemental analysis calcd (%) for $C_{48}H_{38}F_{12}N_8P_2RuS_6$: C 44.0, H 2.92, N 8.55; found: C 44.47, H 3.13, N 8.15.

$[Ru(bpy)(TTF\text{-}dppz)_2](PF_6)_2$ (**2**): A solution of $[Ru(bpy)(phendione)_2](PF_6)_2$ (100 mg, 0.056 mmol) and 5,6-diamino-2-[4,5-bis(propylthio)-1,3-dithio-2-ylidene]benzo[*d*]-1,3-dithiol (48 mg, 0.12 mmol) in ethanol (10 mL) was heated at reflux for 16 h under argon until complete consumption of the starting material was detected. After cooling to room temperature, the precipitate was filtered off. Aqueous potassium hexafluorophosphate was added to the filtrate. The crude precipitate was washed twice with water and once with diethyl ether and then purified by chromatography on a column packed with basic alumina ($MeOH/CH_2Cl_2$, gradient from 0:100 to 5:95). The fractions containing the pure complex were evaporated to dryness and recrystallised by the slow evaporation of a solution in CH_2Cl_2/hexane (ca. 80:20) to give 20 mg (20%) of analytically pure product. ^{1}H NMR (CD_2Cl_2, 300 MHz): δ = 9.61 [d, ^3J(H,H) = 8.3 Hz, 2H), 9.51 (d, ^3J(H,H) = 8.1 Hz, 2H], 8.41 [d, ^3J(H,H) = 7.9 Hz, 2H], 8.17 [d, ^3J(H,H) = 5.1 Hz, 2H], 8.09–7.89 (m, 10H), 7.80 [d, ^3J(H,H) = 5.4 Hz, 2H], 7.75–7.73 (m, 2H), 7.38–7.33 (m, 2H), 2.76 [t, ^3J(H,H) = 7.2 Hz, 8H], 1.67–1.54 (m, 8H), 0.95 ppm [t, ^3J(H,H) = 7.3 Hz, 12H]; IR (KBr): $\tilde{\nu}$ = 2960, 1605, 1446, 1426, 1345, 1088, 838, 761, 557 cm^{-1}; UV/Vis (CH_2Cl_2): λ_{max} (ε) = 620 (19000), 460 (18000), 380 nm (25000 $M^{-1}cm^{-1}$); ESI-MS *m/z*: 735.00; calcd for $[M-2PF_6]^{2+}$: 735.00; elemental analysis calcd (%) for $C_{66}H_{52}F_{12}N_{10}P_2RuS_{12}$: C 45.02, H 2.98, N 7.95; found: C 44.73, H 3.01, N 7.56.

$[Ru(TTF\text{-}dppz)_3](PF_6)_2$ (**3**): A solution of $[Ru(phendione)_3](PF_6)_2$ (44 mg, 0.043 mmol) and 5,6-diamino-2-[4,5-bis(propylthio)-1,3-dithio-2-ylidene]benzo[*d*]-1,3-dithiol (70 mg, 0.16 mmol) in ethanol (5 mL) was heated at reflux for 16 h under argon until complete consumption of the starting material was detected. After cooling to room temperature, the precipitate was filtered off. Aqueous potassium hexafluorophosphate was added to the filtrate. The crude precipitate was washed twice with water and once with diethyl ether and then purified by chromatography on a column packed with basic alumina ($MeOH/CH_2Cl_2$, gradient from 0:100 to 5:95). The fractions containing the pure complex were evaporated to dryness and recrystallised by the slow evaporation of a solution in CH_2Cl_2/hexane (ca. 80:20) to give 30 mg (32%) of analytically pure product. ^{1}H NMR (CD_2Cl_2, 300 MHz): δ = 9.58 [d, ^3J(H,H) = 8.7 Hz, 6H], 8.18 [d, ^3J(H,H) = 5.1 Hz, 6H], 8.11 (s, 6H), 7.82–7.78 (m, 6H), 2.76 [t, ^3J(H,H) = 7.2 Hz, 12H], 1.67–1.54 (m, 12H), 0.95 ppm [t, ^3J(H,H) = 7.2 Hz, 18H] IR (KBr): $\tilde{\nu}$ = 2959, 1603, 1446, 1426, 1351, 840, 760, 555 cm^{-1}; UV/Vis (CH_2Cl_2): λ_{max} (ε) = 620 (25000), 460 (18000), 380 nm (40000 $M^{-1}cm^{-1}$); ESI-MS: *m/z*: 960.98; calcd for $[M-2PF_6]^{2+}$: 960.98; elemental analysis calcd (%) for $C_{84}H_{66}F_{12}N_8P_2RuS_6$: C 45.62, H 3.01, N 7.60; found: C 45.41, H 2.75, N 7.26.

Acknowledgements

This work was supported by the Swiss National Science Foundation (grant No. 200020-107589 and 200020-107423 and COST Action D31) as well as by the ESF program SONS (NANOSYN).

Keywords: donor–acceptor systems · electron transfer · fulvalenes · N ligands · ruthenium

[1] a) J. Yamada, T. Sugimoto, *TTF Chemistry. Fundamentals and Applications of Tetrathiafulvalene*, Springer Verlag, Berlin, **2004**; b) T. Otsubo, K. Takimiya, *Bull. Chem. Soc. Jpn.* **2004**, *77*, 43–58.

[2] a) M. Bendikov, F. Wudl, D. F. Perepichka, *Chem. Rev.* **2004**, *104*, 4891–4945; b) M. C. Díaz, B. M. Illescas, N. Martin, I. F. Perepichka, M. R. Bryce, E. Levillain, R. Viruela, E. Ortí, *Chem. Eur. J.* **2006**, *12*, 2709–2721; c) M. B. Nielsen, C. Lomholt, J. Becher, *Chem. Soc. Rev.* **2000**, *29*, 153–164; d) J. L. Segura, N. Martín, *Angew. Chem.* **2001**, *113*, 1416–1455; *Angew. Chem. Int. Ed.* **2001**, *40*, 1372–1409.

[3] a) F. Dumur, N. Gautier, N. Gallego-Planas, Y. Sahin, E. Levillain, N. Mercier, P. Hudhomme, M. Masino, A. Girlando, V. Lloveras, J. Vidal-Gancedo, J. Veciana, C. Rovira, *J. Org. Chem.* **2004**, *69*, 2164–2177; b) I. Fuks-Janczarek, J. Luc, B. Sahraoui, F. Dumur, P. Hudhomme, J. Berdowski, I. V. Kityk, *J. Phys. Chem. B* **2005**, *109*, 10179–10183.

[4] a) C. Loosli, C. Y. Jia, S-X. Liu, M. Haas, M. Dias, E. Levillain, A. Neels, G. Labat, A. Hauser, S. Decurtins, *J. Org. Chem.* **2005**, *70*, 4988–4992; b) J. O. Jeppesen, J. Becher, *Eur. J. Org. Chem.* **2003**, 3245–3266; c) H. C. Li, J. O. Jeppesen, E. Levillain, J. Becher, *Chem. Commun.* **2003**, 846–847.

[5] a) S-X. Liu, S. Dolder, P. Franz, A. Neels, H. Stoeckli-Evans, S. Decurtins, *Inorg. Chem.* **2003**, *42*, 4801–4803; b) C. Jia, S-X. Liu, C. Ambrus, A. Neels, G. Labat, S. Decurtins, *Inorg. Chem.* **2006**, *45*, 3152–3154; c) S. Dolder, S-X. Liu, E. Beurer, L. Ouahab, S. Decurtins, *Polyhedron* **2006**, *25*, 1514–1518; d) S-X. Liu, S. Dolder, M. Pilkington, S. Decurtins, *J. Org. Chem.* **2002**, *67*, 3160–3162; e) T. Devic, N. Avarvari, P. Batail, *Chem. Eur. J.* **2004**, *10*, 3697–3707; f) T. Devic, D. Rondeau, Y. Şahin, E. Levillain, R. Clérac, P. Batail, N. Avarvari, *Dalton Trans.* **2006**, 1331–1337; g) A. Ota, L. Ouahab, S. Golhen, O. Cador, Y. Yoshida, G. Saito, *New J. Chem.* **2005**, *29*, 1135–1140; h) K. Hervé, S-X. Liu, O. Cador, S. Golhen, Y. Le Gal, A. Bousseksou, H. Stoeckli-Evans, S. Decurtins, L. Ouahab, *Eur. J. Inorg. Chem.* **2006**, 3498–3502.

[6] A. Kobayashi, E. Fujiwara, H. Kobayashi, *Chem. Rev.* **2004**, *104*, 5243–5264, and references therein.

[7] a) Q-Y. Zhu, G-Q. Bian, Y. Zhang, J. Dai, D-Q. Zhang, W. Lu, *Inorg. Chim. Acta* **2006**, *359*, 2303–2308; b) J. Massue, N. Bellec, S. Chopin, E. Levillain, T. Roisnel, R. Clérac, D. Lorcy, *Inorg. Chem.* **2005**, *44*, 8740–8748; c) N. Bellec, D. Lorcy, *Tetrahedron Lett.* **2001**, *42*, 3189–3191.

[8] a) P. Pellon, G. Gachot, J. Le Bris, S. Marchin, R. Carlier, D. Lorcy, *Inorg. Chem.* **2003**, *42*, 2056–2060; b) B. W. Smucker, K. R. Dunbar, *J. Chem. Soc. Dalton Trans.* **2000**, 1309–1315; c) E. Cerrada, C. Diaz, M. C. Diaz, M. B. Hursthouse, M. Laguna, M. E. Light, *J. Chem. Soc. Dalton Trans.* **2002**, 1104–1109; d) T. Devic, P. Batail, M. Fourmigue, N. Avarvari, *Inorg. Chem.* **2004**, *43*, 3136–3141; e) M. Guerro, T. Roisnel, P. Pellon, D. Lorcy, *Inorg. Chem.* **2005**, *44*, 3347–3355; f) G. Gachot, P. Pellon, T. Roisnel, D. Lorcy, *Eur. J. Inorg. Chem.* **2006**, 2604–2611.

[9] S-X. Liu, C. Ambrus, S. Dolder, A. Neels, S. Decurtins, *Inorg. Chem.* **2006**, *45*, 9622–9624.

[10] C. Jia, S-X. Liu, C. Tanner, C. Leiggener, A. Neels, L. Sanguinet, E. Levillain, S. Leutwyler, A. Hauser, S. Decurtins, *Chem. Eur. J.* **2007**, *13*, 3804–3812.

[11] a) L. Spiccia, G. B. Deacon, C. M. Kepert, *Coord. Chem. Rev.* **2004**, *248*, 1329–1341; b) J. G. Vos, J. M. Kelly, *Dalton Trans.* **2006**, 4869–4883; c) A. Juris, V. Balzani, F. Barigelletti, S. Campagna, P. Belser, A. Von Zelewski, *Coord. Chem. Rev.* **1988**, *84*, 85–277; d) J. Rusanova, S. Decurtins, E. Rusanov, H. Stoeckli-Evans, S. Delahaye, A. Hauser, *J. Chem. Soc. Dalton Trans.* **2002**, 4318–4320; e) M. Hissler, A. Harriman, A. Khatyr, R. Ziessel, *Chem. Eur. J.* **1999**, *5*, 3366–3381; f) M. Galletta, F. Puntoriero, S. Campagna, C. Chiorboli, M. Quesada, S. Goeb, R. Ziessel, *J. Phys. Chem. A* **2006**,

110, 4348 – 4358; g) D. V. Kozlov, D. S. Tyson, C. Goze, R. Ziessel, F. N. Castellano, *Inorg. Chem.* **2004**, *43*, 6083 – 6092.

[12] a) V. Balzani, F. Scandola, *Supramolecular Photochemistry*, Horwood, Chichester, **1991**; b) V. Balzani, A. Juris, M. Venturi, S. Campagna, S. Serroni, *Chem. Rev.* **1996**, *96*, 759 – 834; c) L. Sun, L. Hammarström, B. Åkermark, S. Styring, *Chem. Soc., Rev.* **2001**, *30*, 36 – 49; d) R. Ballardini, V. Balzani, A. Credi, M. T. Gandolfi, M. Venturi, *Acc. Chem. Res.* **2001**, *34*, 445 – 455; e) F. Barigelletti, L. Flamigni, *Chem. Soc., Rev.* **2000**, *29*, 1 – 12; f) D. Pomeranc, V. Heitz, J-C. Chambron, J-P. Sauvage, *J. Am. Chem. Soc.* **2001**, *123*, 12215 – 12221; g) C. N. Fleming, K. A. Maxwell, J M. DeSimone, T. J. Meyer, J. M. Papanikolas, *J. Am. Chem. Soc.* **2001**, *123*, 10336 – 10347; h) E. R. Batista, R. L. Martin, *J. Phys. Chem. A* **2005**, *109*, 3128- 3133; i) M. K. Brennaman, J. H. Alstrum-Acevedo, C. N. Fleming, P. Jang, T. J. Meyer, J. M. Papanikolas, *J. Am. Chem. Soc.* **2002**, *124*, 15094 – 15098.

[13] a) Q. Wang, S. M. Zakeeruddin, M. K. Nazeeruddin, R. Humphry-Baker, M. Grätzel, *J. Am. Chem. Soc.* **2006**, *128*, 4446 – 4452; b) P. Wang, C. Klein, R. Humphry-Baker, S. M. Zakeeruddin, M. Grätzel, *J. Am. Chem. Soc.*, **2005**, *127*, 808 – 809; c) M. K. Nazeeruddin, Q. Wang, L. Cevey, V. Aranyos, P. Liska, E. Figgemeier, C. Klein, N. Hirata, S. Koops, S. A. Haque, J. R. Durrant, A. Hagfeldt, A. B. P. Lever, M. Grätzel, *Inorg. Chem.* **2006**, *45*, 787 – 797; d) D. Kuang, C. Klein, H. J. Snaith, J-E. Moser, R. Humphry-Baker, P. Comte, S. M. Zakeeruddin, M. Grätzel, *Nano Lett.* **2006**, *6*, 769 – 773.

[14] a) M. Cusumano, M. L. Di Pietro, A. Giannetto, *Inorg. Chem.* **2006**, *45*, 230 – 235; b) A. E. Friedman, J.-C. Chambron, J.-P. Sauvage, N. J. Turro, J. K. Barton, *J. Am. Chem. Soc.* **1990**, *112*, 4960 – 4962; c) R. M. Hartshorn, J. K. Barton, *J. Am. Chem. Soc.* **1992**, *114*, 5919 – 5925; d) C. Hiort, P. Lincoln, B. Nordén, *J. Am. Chem. Soc.* **1993**, *115*, 3448 – 3454.

[15] a) Y. Liu, A. Chouai, N. N. Degtyareva, D. A. Lutterman, K. R. Dunbar, C. Turro, *J. Am. Chem. Soc.* **2005**, *127*, 10796 – 10797; b) E. D. A. Stemp, M. R. Arkin, J. K. Barton, *J. Am. Chem. Soc.* **1995**, *117*, 2375 – 2376; c) C. G. Coates, L. Jacquet, J. J. McGarvey, S. E. J. Bell, A. H. R. Al-Obaidi, J. M. Kelly, *J. Am. Chem. Soc.* **1997**, *119*, 7130 – 7136.

[16] a) J. E. Dickeson, L. A. Summers, *Aust. J. Chem.* **1970**, *23*, 1023 – 1027; b) C. M. Dupureur, J. K. Barton, *Inorg. Chem.* **1997**, *36*, 33 – 43; c) A. Kleineweischede, J. Mattay, *J. Organomet. Chem.* **2006**, *691*, 1834 – 1844.

[17] S. Campagna, S. Serroni, F. Puntoriero, F. Loiseau, L. De Cola, C. J. Kleverlaan, J. Becher, A. P. Sørensen, P. Hascoat, N. Thorup, *Chem. Eur. J.* **2002**, *8*, 4461 – 4469.

[18] a) M. R. Bryce, *Adv. Mater.* **1999**, *11*, 11 – 23; b) K. Schaumburg, J. M. Lehn, V. Goulle, S. Roth, H. Byrne, S. Hagen, J. Poplawski, K. Brunfeldt, K. Bechghaard, T. Bjørnholm, P. Frederiksen, M. Jørgensen, K. Lerstrup, P. Sommer-Larsen, O. Goscinski, J. L. Calais, L. Eriksson, *Nanostructures Based on Molecular Materials* (Eds.: W. Göpel, C. Ziegler), VCH, Weinheim **1992**, pp. 153 – 172.

[19] a) S-X. Liu, A. Neels, H. Stoeckli-Evans, S. Decurtins, *Phosphorus Sulfur Silicon Relat. Elem.* **2005**, *180*, 1469 – 1470; b) K. Sako, Y. Misaki, M. Fujiwara, T. Maitani, K. Tanaka, H. Tatemitsu, *Chem. Lett.* **2002**, 592 – 593.

[20] N. Komatsuzaki, R. Katoh, Y. Himeda, H. Sugihara, H. Arakawa, K. Kasuga, *J. Chem. Soc. Dalton Trans.* **2000**, 3053 – 3054.

[21] C-Y. Jia, S-X. Liu, C. Tanner, C. Leiggener, L. Sanguinet, E. Levillain, S. Leutwyler, A. Hauser, S. Decurtins, *Chem. Commun.* **2006**, 1878 – 1880.

[22] J. Ulstrup, J. Jortner, *J. Chem. Phys.* **1975**, *63*, 4358.

[23] a) C. Katan, *J. Phys. Chem. A* **1999**, *103*, 1407 – 1413; b) B. J. Matthewson, A. Flood, M. I. J. Polson, C. Armstrong, D. L. Phillips, K. C. Gordon, *Bull. Chem. Soc. Jap.* **2002**, *75*, 933 – 942.

[24] a) J. A. Treadway, B. Loeb, R. Lopez, P. A. Anderson, F. R. Keene, T. J. Meyer, *Inorg. Chem.* **1996**, *35*, 2242 – 2246; b) M. Arias, J. Concepción, I. Crivelli, A. Delgadillo, R. Díaz, A. Francois, F. Gajardo, R. López, A. M. Leiva, B. Loeb, *Chem. Phys.* **2006**, *326*, 54 – 70.

[25] R. M. Hartshorn, J. K. Barton, *J. Am. Chem. Soc.* **1992**, *114*, 5919 – 5925.

[26] F. E. Lytle, D. M. Hercules, *J. Am. Chem. Soc.* **1969**, *91*, 253 – 257.

[27] S. Wallin, J. Davidsson, J. Modin, L. Hammarström, *J. Phys. Chem. A* **2005**, *109*, 4697 – 4704.

[28] J. Fees, W. Kaim, M. Moscherosch, W. Matheis, J. Klima, M. Krejcik, S. Zalis, *Inorg. Chem.* **1993**, *32*, 166 – 174.

[29] G. Sprintschnik, H. W. Sprintschnik, P. P. Kirsch, D. Whitten, *J. Am. Chem. Soc.* **1977**, *99*, 4947 – 4954.

[30] S. D. Bergman, M. Kohl, *Inorg. Chem.* **2005**, *44*, 1647 – 1654.

[31] J. Leveque, B. Elias, C. Moucheron, A. Kirsch-De Mesmaeker, *Inorg. Chem.* **2005**, *44*, 393 – 400.

Received: January 26, 2007
Revised: April 19, 2007
Published online on May 29, 2007

